Conformational Change in the NADP(H) Binding Domain of Transhydrogenase Defines Four States[†,‡]

Vidyasankar Sundaresan, Mutsuo Yamaguchi, Justin Chartron, and C. David Stout*

Department of Molecular Biology, 10550 North Torrey Pines Road, The Scripps Research Institute, La Jolla, California 92037

Received June 12, 2003; Revised Manuscript Received August 13, 2003

ABSTRACT: Proton-translocating transhydrogenase (TH) couples direct and stereospecific hydride transfer between NAD(H) and NADP(H), bound to soluble domains dI and dIII, respectively, to proton translocation across a membrane bound domain, dII. The reaction occurs with proton-gradient coupled conformational changes, which affect the energetics of substrate binding and interdomain interactions. The crystal structure of TH dIII from *Rhodospirillum rubrum* has been determined in the presence of NADPH (2.4 Å) and NADP (2.1 Å) (space group $P6_122$). Each structure has two molecules in the asymmetric unit, differing in the conformation of the NADP(H) binding loop D. In one molecule, loop D has an open conformation, with the B face of (dihydro)nicotinamide exposed to solvent. In the other molecule, loop D adopts a hitherto unobserved closed conformation, resulting in close interactions between NADP(H) and side chains of the highly conserved residues, βSer405, βPro406, and βIle407. The conformational change shields the B face of (dihydro)nicotinamide from solvent, which would block hydride transfer in the intact enzyme. It also alters the environments of invariant residues βHis346 and βAsp393. However, there is little difference in either the open or the closed conformation upon change in oxidation state of nicotinamide, i.e., for NADP vs. NADPH. Consequently, the occurrence of two loop D conformations for both substrate oxidation states gives rise to four states: NADP-open, NADP-closed, NADPH-open, and NADPH-closed. Because these states are distinguished by protein conformation and by net charge they may be important in the proton translocating mechanism of intact TH.

Transhydrogenase (TH)[1] is a homodimeric integral membrane enzyme found in the prokaryotic cell membrane and eukaryotic inner mitochondrial membrane. The monomer has a molecular mass of ∼110 kDa (*1*−*4*) and consists of a soluble NAD(H) binding domain (dI, 400−430 residues), a membrane-bound proton-translocating domain (dII, 360−400 residues), and a soluble NADP(H) binding domain (dIII, ∼200 residues), with linkers of variable length connecting the domains. Both dI and dIII occur on the same side of the membrane in the prokaryotic cytosol or the eukaryotic mitochondrial matrix. TH couples proton translocation across dII to hydride ion transfer between NAD(H) and NADP(H), with a H^+/H^- stoichiometry of $n = 1$ in the equation:

$$\mathrm{NADH} + \mathrm{NADP} + n\mathrm{H^+_{out}} \rightleftharpoons \mathrm{NAD} + \mathrm{NADPH} + n\mathrm{H^+_{in}} \quad (1)$$

The hydride transfer is stereospecific, between the 4A position of NAD(H) and the 4B position of NADP(H), and direct, involving no reactive intermediates. Although the three-dimensional arrangement of domains in the intact enzyme is unknown, the soluble domains must interact to bring the (dihydro)nicotinamide rings of NAD(H) and NADP(H) into direct contact (∼3 Å) with each other. As the difference between the redox potentials of NAD(H) and NADP(H) is negligible, it is expected that in both forward and reverse directions (eq 1), proton flux across the membrane-spanning domain is coupled to changes in the conformations of soluble domains of TH (*1*−*4*).

In eukaryotic mitochondria, the three domains of TH comprise a single polypeptide chain, in the order dI−dII−dIII from the NH_2- to COOH-terminus. Protozoan species (*Eimeria tenella* and *Entamoeba histolytica*) also have a single polypeptide, but with a shuffled arrangement of the three domains (*5*). In prokaryotic cells, TH typically consists of two or three subunits: *Escherichia coli* TH has an α subunit that comprises dI and an N-terminal portion of dII, and a β subunit that contains the rest of dII and all of dIII. In *Rhodospirillum rubrum*, the α subunit is expressed as two polypeptides, while the β subunit corresponds to those in *E. coli* and other prokaryotes (Figure 1a). An alignment of dIII residues from 51 prokaryotic and eukaryotic species is given in the Supporting Information (Figure S1).

The soluble domains have been expressed in *E. coli* for biochemical and structural investigations. TH dIII is expressed as a monomer with one molecule of NADP(H) bound, while TH dI is expressed as a dimer with one molecule of NAD(H) bound (*5*). A reconstituted mixture of dI and dIII from the same species or from different species

[†] This research was supported by NIH Grant GM61545.

[‡] PDB deposition codes: 1PNO (NADP complex) and 1PNQ (NADPH complex).

* Corresponding author: tel.: 858-784-8738; fax: 858-784-2857; e-mail: dave@scripps.edu.

[1] Abbreviations: TH, transhydrogenase; NAD, nicotinamide adenine dinucleotide; NADH, dihydronicotinamide adenine dinucleotide; NADP, nicotinamide adenine dinucleotide phosphate; NADPH, dihydronicotinamide adenine dinucleotide phosphate; AcPyAD, acetylpyridine adenine dinucleotide; IAEDANS, 5-((((2-iodoacetyl)amino)ethyl)amino naphthalene-1-sulfonic acid); MIANS, 2-(4′-maleimidylanilino)naphthalene-6-sulfonic acid; NEM, *N*-ethylmaleimide; DTT, dithiothreotol; PMSF, phenylmethylsulfonyl fluoride.

10.1021/bi035006q CCC: $25.00
Published on Web 10/01/2003

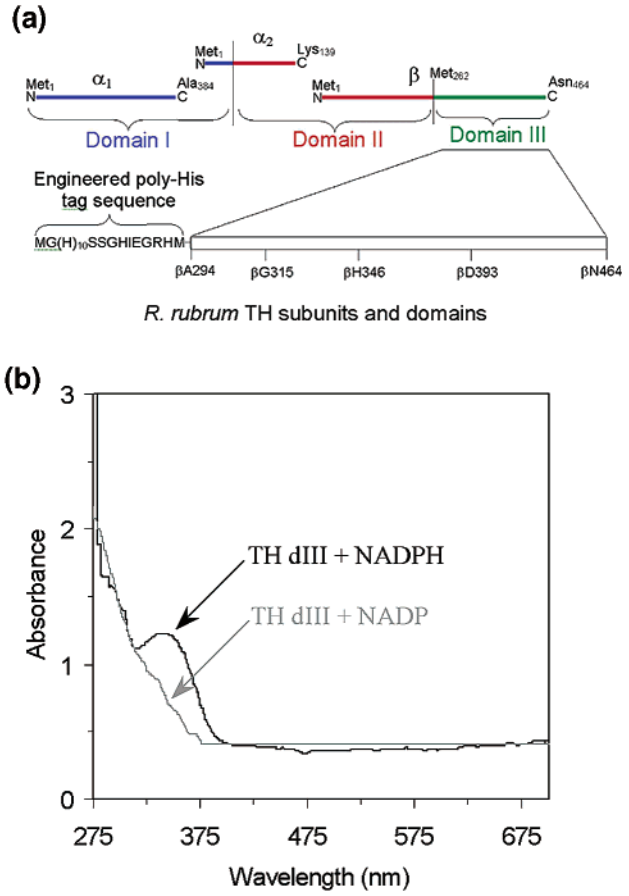

FIGURE 1: (a) Arrangement of the three tranhydrogenase (TH) domains (I, II, III) in the *R. rubrum* enzyme, which is comprised of three subunits, α_1, α_2, and β. Domains I and III bind NAD(H) and NADP(H), respectively, and domain II contains the proton channel and is membrane intercalated. For crystallization of domain III residues 294−464 of the β subunit were expressed as a construct engineered to have a 22-residue N-terminal sequence containing a 10-residue poly-His tag. (b) UV−visible absorbance spectra of crystals of domain III of *R. rubrum* TH grown with the NADP complex (gray line) and with the NADPH complex (black line). The crystals containing NADPH show a characteristic absorbance at ~340 nm for dihydronicotinamide, which is absent in crystals containing NADP. Similar spectra were obtained for at least five crystal specimens of both the NADP and NADPH complexes.

can catalyze hydride transfer between NAD(H) and NADP(H) in solution (*5*−*8*) in the absence of dII, the proton translocating domain. The structure of TH dIII bound to NADP has been determined crystallographically for the bovine (*9*) and human (*10*) proteins and by using NMR methods for the *R. rubrum* protein (*11*). In these structures, NADP is bound such that the B face of the nicotinamide ring is exposed to solvent. Crystal structures have also been determined for TH dI from *R. rubrum*, in the presence of NAD (*12*), in the presence of NADH, and in the absence of substrate (*13*). These structures show interdigitating contacts and an extensive network of interactions between the two closely associated monomers of dI with NAD(H) bound such that the A face of its (dihydro)nicotinamide ring is exposed to solvent. One molecule of NAD(H) is bound per dI dimer, consistent with the experimentally observed "half-the-sites-reactivity" profile of the enzyme (*14*). A "heterotrimer" cocrystal structure has been reported (*15*), containing a dIII monomer with NADP bound, in association with a dI dimer with one molecule of NAD bound. In this structure, both substrates are in the oxidized state and NAD is bound in the dI monomer farther from dIII and NADP. The structures of the dI dimer and the dIII monomer in this complex are very similar to those observed in crystal structures of the individual domains.

The available structures of TH dIII (*9*−*11*, *15*) are all similar to one another. However, other experiments indicate that significant conformational change, required for proton pumping in the absence of a net redox potential (*1*−*3*), occurs in some component of dIII. For example, tryptic cleavage of intact (*16*) and proteinase K-bisected (*17*) bovine TH is accelerated in the presence of NADPH compared to NADP, but largely unaffected by either NAD or NADH. These and other data indicate that the oxidation state of NADP(H) bound to dIII has a significant effect either on the conformation of dIII and/or on the interactions between dI and dIII (*18*−*20*). Incorporating this information, the crystal structure of the "heterotrimeric" complex, and extensive kinetic data, an "alternating site, binding change mechanism" has been proposed for TH (*3*), which entails large changes in the relative arrangement of dI and dIII. Two loops in dIII in association with NADP(H) have been specifically implicated in conformational change. Mutagenesis studies, fluorescence resonance energy transfer experiments, and kinetic studies (*18*−*20*) with the *E. coli* and *R. rubrum* proteins indicate that loop D of dIII mediates interactions with dI, and that loop E accommodates NADP(H) binding and release.

In this paper, we report the first structure of dIII bound to NADPH. *R. rubrum* dIII bound to NADP was crystallized under similar conditions. In each case, the asymmetric unit in the crystal form obtained contains two molecules: in one the conformation of loop D is "open", as observed previously (*9*−*11*, *15*) with the B face of the (dihydro)nicotinamide ring exposed to solvent; in the other it is "closed", blocking this face from solvent. The closed conformation involves large movement of loop D residues. Surprisingly, however, the presence of NADPH vs. NADP does not affect the conformation of either the open or closed forms. Consequently, the structures define four states of dIII potentially relevant to the TH mechanism: NADP-open, NADP-closed, NADPH-open, and NADPH-closed.

EXPERIMENTAL PROCEDURES

Protein Expression and Purification. Recombinant *R. rubrum* TH dIII was expressed in *E. coli* and purified as described (*5*). The purified protein has an engineered N-terminal histidine tag preceding residue βA294 (Figure 1a) and contains both NADP and NADPH in the ratio 4:6. The NADPH form of dIII was prepared by incubating purified dIII with a 10-fold excess of NADPH, followed by gel filtration on Sephadex G-50 to remove excess nucleotides. Expressed *R. rubrum* dIII has a high avidity for NADPH vs. NADP (*5*). The NADP form of dIII was prepared by incubating purified dIII with a catalytic amount of *R. rubrum* dI and AcPyAD to oxidize bound NADPH (*6*). Extra nucleotides and the dI protein were removed by DEAE-Sephadex column chromatography. The UV−visible spectrum confirmed the oxidation state for each preparation. Subsequently, single-crystal spectra confirmed the oxidation state of the nicotinamide cofactors in the crystals (Figure 1b). Protein preparations were exchanged into D_2O using a

Sephadex G-50 column equilibrated with 20 mM Tris·HCl buffer adjusted to pH* 8.2 containing 0.8 mM DTT, 0.4 mM PMSF, and 1 mM NADP or 1mM NADPH. Protein samples were concentrated to ~14 mg/mL in a Centricon-10 concentrator.

Crystallization and Data Collection. Crystallization was done by vapor diffusion with 1 μL of protein solution in D_2O mixed with 1 μL of the reservoir solution in H_2O. Conditions were identified from the "footprint screen" (*21*) and refined. Hexagonal bipyramidal crystals of *R. rubrum* dIII with NADPH bound were obtained with a reservoir solution consisting of 0.6 M $(NH_4)_2SO_4$ and 30 mM sodium citrate buffer at pH 5.5. Crystal nucleation and growth occurred at 8 °C in 2−3 days. The estimated pH in the crystallization drops was 6.5−6.7, based on measurements for an equal volume mixture of the buffers in 50% D_2O at 8 °C, and based on indicator dyes for 1 μL aliquots of the drops. For dIII with NADP bound, the reservoir solution consisted of 1.4 M $(NH_4)_2SO_4$ and 75 mM sodium citrate buffer at pH 5.5. A heavy microcrystalline precipitate formed at 24 °C overnight, from which hexagonal bipyramidal crystals grew over 4−5 days. The estimated pH in these crystallization drops was 5.7−5.8, based on measurements for an equal volume mixture of the buffers in 50% D_2O at 24 °C, and based on indicator dyes for 1 μL aliquots of the drops. For cryoprotection prior to X-ray data collection, crystals were soaked in synthetic mother liquor containing 25% glycerol added to the reservoir solution in H_2O. Data were collected at 100 K at the Stanford Synchrotron Radiation Laboratory (SSRL) beam lines 9-2 and 11-1, and processed with CCP4 (*22*) programs (Table 1).

Single-Crystal Spectrophotometry. The oxidation state of NADP(H) in TH dIII crystals was investigated by collecting single-crystal spectra in the UV−visible range (Figure 1b). Spectra were collected in the wavelength range 260−700 nm from six crystals with NADP bound and five crystals with NADPH bound. Crystals were soaked in the cryoprotecting solution for ~10 min to soak out unbound NADP(H). The single-crystal microspectrophotometer was equipped with a Mercury−Xenon arc lamp light source, optical components to focus the incident beam to 5 μ, and linear CCD array detector (E. Getzoff, personal communication). Crystals were mounted on nylon cryoloops, transferred to a goniometer head, positioned with translation stages, viewed with a binocular microscope, and maintained at 100 K with a liquid N_2 supplied cryostream. Crystals were positioned to optimize absorbance at ~340 nm. Due to variable absorption by the crystals, the incident beam intensity and count time were then adjusted to obtain comparable absorbance over 400−700 nm for different specimens. For comparison, reference background spectra were measured for each incident intensity and count time.

Molecular Replacement, Model Building, and Refinement. A molecular replacement solution, using the *R. rubrum* domain III from the "heterotrimer" structure (*15*) as the search model, was found in the σ_A likelihood based program BEAST (*23*) using data truncated to 3.5 Å resolution. The best three solutions from the first rotation function search were used for translation function searches and solutions were monitored both for log-likelihood gain and the number of members in each solution cluster. The first copy of the molecule was located and fixed at its corresponding Eulerian angles and fractional coordinates before carrying out rotation searches for the second copy and subsequent translation searches. The log-likelihood gains and the number of members associated with the best solutions are given in Table 1. This molecular replacement solution, containing two molecules in the asymmetric unit, was used as a search model for the dataset obtained for crystals containing NADPH.

Table 1: Crystallographic Analysis

	Crystals	
complex	NADP	NADPH
no. of crystals	1	1
space group	$P6_122$	$P6_122$
unit cell (a,b,c)[a] (Å)	117.9 × 117.9 × 211.3	118.3 × 118.3 × 212.8
	Data Collection	
SSRL beam line	11-1	9-1
wavelength (Å)	0.965	0.979
resolution range (Å)	29.0−2.1	19.7−2.4
total observations	172,564	317,639
unique reflections > 0.0 σF	50,245	34,800
redundancy	3.4	9.1
completeness	98.5%	99.0%
$\langle I/\sigma_I \rangle$[b]	10.7 (1.2)	17.3 (1.4)
R_{symm} (I)[b]	0.076 (0.786)	0.085 (0.635)
	Molecular Replacement[c]	
	Log Likelihood Gain	Number
1st molecule	242.1	45
	25.3	7
2nd molecule	560.6	105
	−1278.2	17
	Refinement	
R-factor	20.9%	21.7%
R_{free} (5% of data)	23.1%	23.1%
rms deviation bonds (Å)	0.007	0.008
rms deviation angles (deg)[d]	1.15	1.15
	No. of Atoms/Avg B-Factor (Å^2)	
protein[e,f]	2698/48.2	2698/48.7
NADP(H)[f]	96/45.8	96/55.7
water molecules	233/52.1	166/63.4

[a] Matthew's coefficient 5.3 Å^3/Da; solvent content 76.6%. [b] Values for the highest resolution shell in parentheses. Values of $\langle I/\sigma_I \rangle < 2.0$ are accepted due to some anisotropy in the diffraction. [c] Statistics for Beast (*23*) calculations for the NADP data set to 3.5 Å resolution. [d] Ramachandran plot for both molecules in the asymmetric unit: 91.7% of residues in most favored regions; 7.7% in allowed regions; 0.6% in generously allowed regions; 0.0% in disfavored regions. [e] Residues 294−464 of the β subunit of *R. rubrum* TH (Figure S1) plus engineered N-terminal residues (nine in chain A and six in chain B). [f] Two molecules in the asymmetric unit (chain A, closed conformation; chain B, open conformation).

The molecular replacement solution gave an R-factor of ~37% (R_{free} ~ 39%) after rigid-body refinement against the data for NADP containing crystals using CNS (*24*). Initial $2|F_o|-|F_c|$ and $|F_o|-|F_c|$ maps showed unambiguous density for NADP in both copies in the asymmetric unit. Two NADP molecules were positioned in the density using Xfit (*25*), and the updated model was subjected to simulated annealing, energy minimization, and isotropic B-factor refinement in CNS. Unbiased σ_A-weighted $2|F_o|-|F_c|$ composite omit maps revealed that the portion of the molecule between the residues βAsn396 and βAsp414 had a substantially different conformation in one of the two molecules in the asymmetric unit. These residues were rebuilt into the electron density using Xfit. The portion of the engineered N-terminal sequence that had well-resolved electron density in the maps was also built

for each copy in the model. The model was further refined by energy minimization and isotropic B-factor refinement in CNS. This process was repeated with the molecular replacement solution obtained for the dataset obtained from an NADPH containing crystal. The final refined models have R of 20.9% (R_{free} 23.1%) for the structure with NADP bound, and R of 21.7% (R_{free} 23.1%) for the structure with NADPH bound. The coordinates have been deposited with the Protein Data Bank with deposition codes, 1PNO and 1PNQ, for the NADP and NADPH containing *R. rubrum* dIII structures, respectively. The models have good geometry with no residues in disallowed regions of the Ramachandran plot (Table 1).

RESULTS

Oxidation State of NADP(H) in the Crystals. Crystals of *R. rubrum* dIII were grown using the NADP and NADPH complexes specifically prepared as described in Experimental Procedures. Single-crystal UV−visible absorbance spectra were measured to confirm the oxidation state of the NADP and NADPH bound in the protein crystals. *R. rubrum* dIII crystals grown in either 5 mM NADP or 5 mM NADPH were soaked in synthetic mother liquor to remove excess unbound reagents and cryoprotected as for X-ray diffraction experiments. Spectra were measured at 100 K using a single-crystal microspectrophotometer (see Experimental Procedures). A distinct peak at 340 nm was observed in all the NADPH-containing crystals, while spectra of NADP-containing crystals exhibited no absorbance at wavelengths beyond the shoulder of the intense protein peak at 280 nm (Figure 1b). This was confirmed in six NADP containing crystals compared to five NADPH containing crystal specimens, and with variation in the incident beam intensity. The absorption at 340 nm in the NADPH containing crystals is consistent with the presence of dihydronicotinamide (*13*, *26*).

Domain III Architecture. In intact TH the N-terminus of dIII is linked to dII, the proton channel domain, while the C-terminus of dIII coincides with the C-terminus of the β subunit of the *R. rubrum* enzyme. The overall structure of dIII in the hexagonal crystal form is similar to that of the bovine (*9*) and human (*10*) dIII crystal structures, and *R. rubrum* dIII in the "heterotrimer" structure (*15*). The nucleotide binding fold contains a central six-stranded, parallel β-sheet flanked by helices and loops (Figure 2a). An additional β strand (β_0) and an α-helix (h_0) precede the first strand of the β-sheet. Two α-helices (h_A and $h_{A'}$) connect strands β_1 and β_2, while strands β_2 and β_3 are connected by a loop and an α-helix (loop B and h_B). The crossover helix (h_C), connecting the two halves of the β sheet ($\beta_3\beta_2\beta_1-\beta_4\beta_5\beta_6$), has mixed α- and 3_{10}-helical character. The protein sequence connecting strands β_4 and β_5 consists largely of the extended loop D, interspersed with short helical turns (h_D, $h_{D'}$, and $h_{D''}$). Strands β_5 and β_6 are connected by another extended loop, loop E, and a short helical turn (h_E). Strand β_6 is followed by a C-terminal α-helix (h_F), which lies between h_0, h_A, and $h_{A'}$.

There is marked conformational difference between the two molecules in the asymmetric unit in both the NADP (Figure 2a) and NADPH (Figure 2b) bound forms of dIII. Each has a distinct conformation for loop D and helix $h_{D'}$, one being "open" and the other "closed". The open conformation leaves the B face of the (dihydro)nicotinamide ring of the substrate exposed to solvent, while the closed conformation blocks this face from solvent. However, comparing the molecules in which the oxidation states of bound nucleotides differ, substantial structural identity is found between the two in the closed conformation (Figure 2c) and the two in the open conformation (Figure 2d).

NADP(H) Conformation. For both oxidation states of the substrate, and for both molecules in the asymmetric unit, NADP(H) electron density is well defined in unbiased $|F_o|-|F_c|$ and σ_A-weighted $2|F_o|-|F_c|$ composite omit maps (Figure 3a). B-factor refinement was consistent with full occupancy in each case. Superposition of all four NADP and NADPH molecules in the final structures (Figure 3b) shows that the conformation does not change significantly with change in oxidation state. In each case, the glycosyl torsion angle for the nicotinamide is syn. As previously observed (*9*), the dinucleotide binds across the C-terminal edge of the β-sheet in an inverted orientation compared to other dinucleotide binding proteins (*27*). Consequently, NADP(H) lies in a cleft flanked by relatively rigid secondary structure elements on one side and flexible loops on the other (Figure 2). The A-face of the (dihydro)nicotinamide packs against hydrophobic residues in loop B and the helical dipole of h_A is oriented toward the dinucleotide phosphates, while the reactive B-face is oriented toward the solvent and the adjoining ribose is adjacent to the flexible loop D.

Loop Conformations. The electron density is equally well defined for both the closed (Figure 4a) and the open (Figure 4b) conformations of loop D in both NADP and NADPH bound dIII. In this region, the protein chain turns from strand β_4 at the invariant residue βGly390 (Figure S1), and goes through a single helical turn (h_D) at the invariant residue βAsp393, which is followed by another invariant residue (βAsn396) and short helix ($h_{D'}$) (Figure 2a). The sequence from βLys400 to βAsp414 comprises loop D, which is followed by another helical turn ($h_{D''}$). Loop D includes the invariant residues βGly409 and βPro411, and the highly conserved residue βMet410, which is replaced by Leu in 1 of 51 species.

The open conformation of loop D is very similar to that observed in previously reported crystal structures (*9*, *10*, *15*). In contrast, the closed conformation is such that conserved residues are repositioned by ~10 Å to interact directly with the B face of the NADP(H) ring. In this conformation, the nicotinamide is sandwiched between loops D and B and both faces are blocked from solvent. In addition, when loop D adopts the closed conformation, the side chains of residues βPro411 to βAsp414 are such that a correlated ~1 Å movement in loop B keeps the nicotinamide occluded from solvent (Figure 2a,b). Hence, in intact TH the open conformation of loop D would be expected to allow direct hydride transfer to proceed, but the closed conformation would block this reaction. Aside from the differences in loops B and D, there is no substantial change in other structural elements of the domain, including loop E, which contributes to NADP(H) binding and extends into the solvent adjacent to loop D.

Conserved Residues. The loop D conformational change from open to closed results in new interactions between the NADP(H) and the side chains of βSer405, βPro406, and βIle407 (Figure 5a). In the open conformation, the Oγ of βSer405 is 11.7 Å away from the ribose 2′-hydroxyl; in the

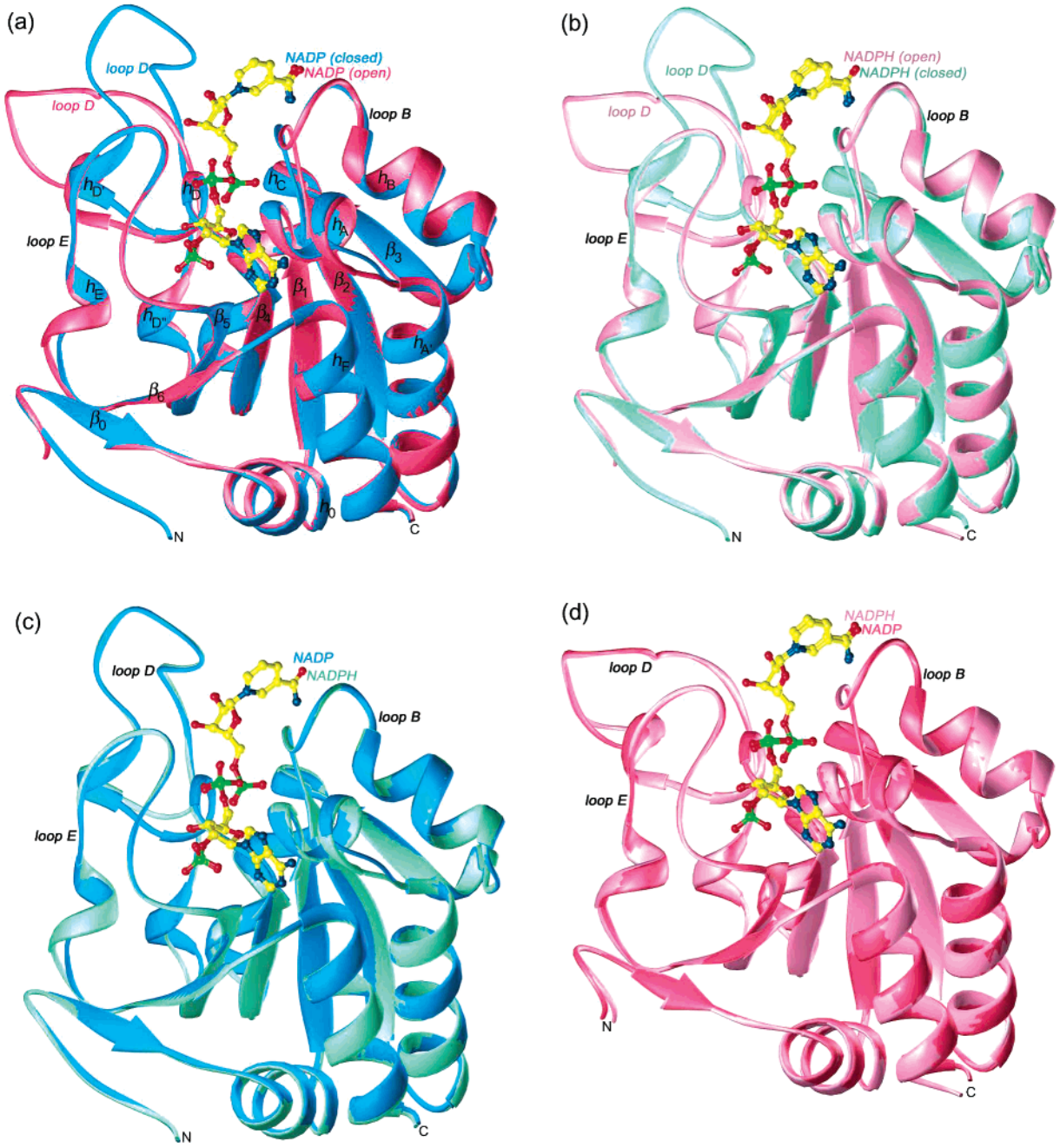

FIGURE 2: Overlaid views of ribbon representations of domain III of *R. rubrum* TH. The two dIII molecules in the asymmetric unit of crystals containing NADP (red, blue) and in crystals containing NADPH (pink, green) are superimposed in (a) and (b), respectively. Secondary structural elements of the domain are labeled in panel a. The molecules with closed and open conformations of loop D, but with different oxidation states of NADP(H) are superimposed in (c) and (d), respectively.

closed conformation it moves to within hydrogen bonding distance, 3.4 Å. The movement also allows βIle407 to stack with the ribose ring, and βPro406 to stack within 3.5 Å of the B face of nicotinamide. These interactions are essentially the same in the reduced NADPH form, except that the βSer405 side chain adopts an alternate rotamer (Figure 5a). βSer405 and βIle407 are conserved in 49 of 51 species (Figure S1), being replaced by Thr and Leu, respectively; βPro406 is slightly more variable, being replaced in eight species. This sequence conservation is consistent with the nature of the additional interactions observed in the closed conformation.

The change from the open to the closed conformation occurs without large internal rearrangement within loop D itself. Hydrogen bonding interactions are maintained at the N- and C-terminal ends of helix $h_{D'}$ and loop D, serving to anchor the conformational change. The amide of βAsn396 hydrogen bonds with the carbonyl of βAsp393 while the side chain of βAsn396 maintains interactions with the main chain at βAla398 and βGlu436 in both conformations (Figure 5b). At the C-terminal end of loop D, a network of hydrogen bonds is retained, involving βHis346, βAsn377, βPro411, βIle412, βLeu413, βAsp414, and βVal394 (Figure 5c). These interactions involve primarily main chain atoms or the side chains of highly conserved residues. In general, the interactions involving either end of loop D correlate very strongly with sequence conservation (Figure S1).

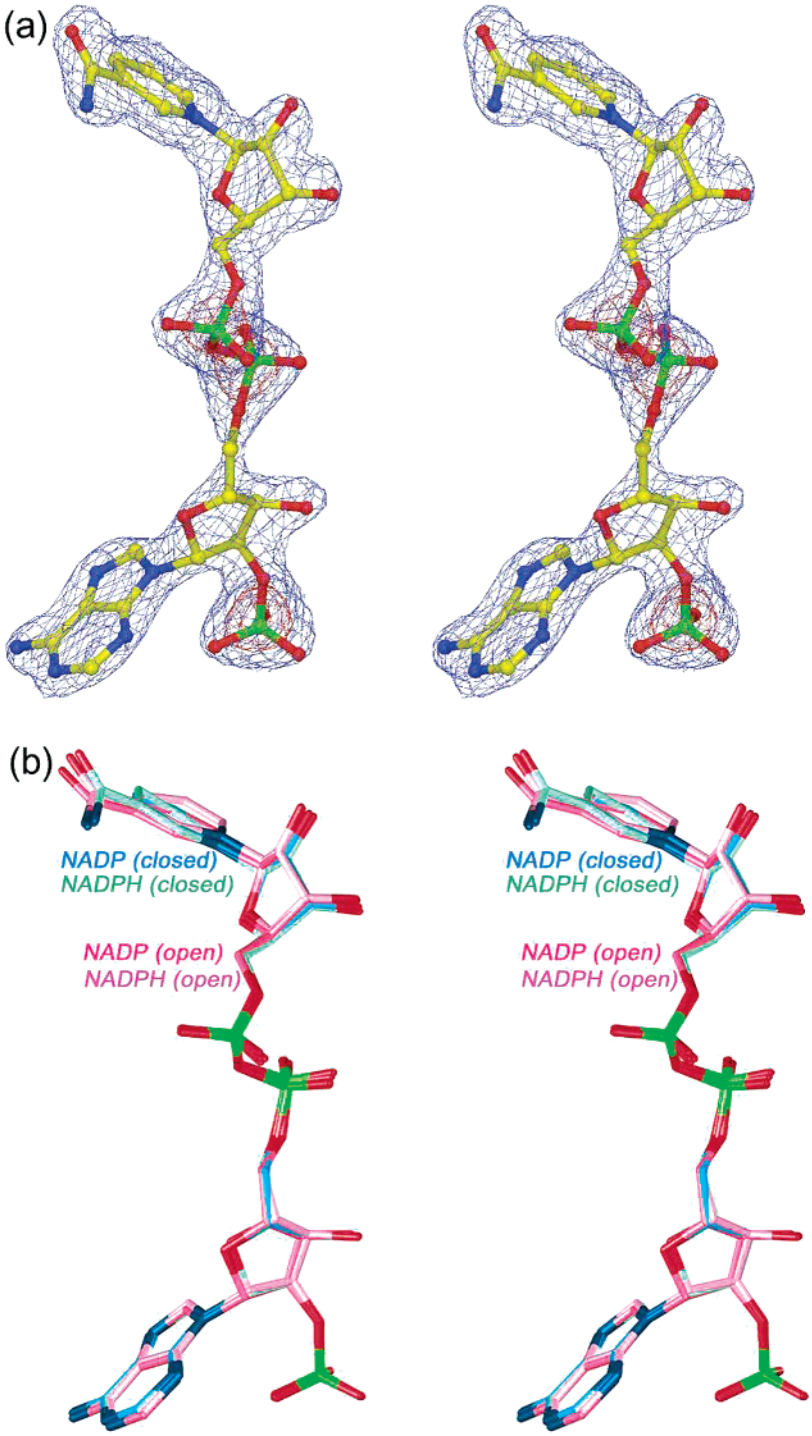

FIGURE 3: Binding conformation of NADP and NADPH in *R. rubrum* dIII. (a) Stereoview of NADP bound to dIII with loop D in the closed conformation and its unbiased σ_A-weighted $2|F_o|-|F_c|$ electron density at 2.1 Å resolution, contoured at 4 and 6σ. (b) Stereoview of the superimposition of both NADP and both NADPH molecules from the final refined structures.

Environment of βAsp393. This invariant residue at the end of strand β_4 hydrogen bonds with the nicotinamide ribose (*9*, *10*; Figure 6a). The change in conformation of helix $h_{D'}$ and loop D results in exchange of the hydrophobic residues adjacent to βAsp393, but the position of this side chain is unaffected (Figure 5b,c). In the open conformation, the side chains of βIle407 and βMet410 pack near βAsp393 (Figure 6a). When loop D changes to the closed conformation, βAla399 moves into the space occupied by βIle407, βIle407 moves into the space occupied by βMet410, and βMet410 moves away, i.e., Ile, Met → Ala, Ile (Figure 6a). In both conformations, βAsp393 retains hydrogen bonds with the 3′-hydroxyl of the nicotinamide ribose and the amide of the loop E residue βAla433 (Figure 6a). Despite the change in packing environment, the solvent exposure of βAsp393 is not significantly altered. βAla399, βIle407, βMet410, and βAla433 are highly conserved residues (Figure S1).

Environment of βHis346. This residue occurs within the invariant domain III sequence His^{346}ProValAlaGlyArg(Met/Leu)ProGly of the β subunit (Figure S1), which comprises loop B (Figure 2a). In this case, the conformational change in loop D results in a distinct change in the environment of

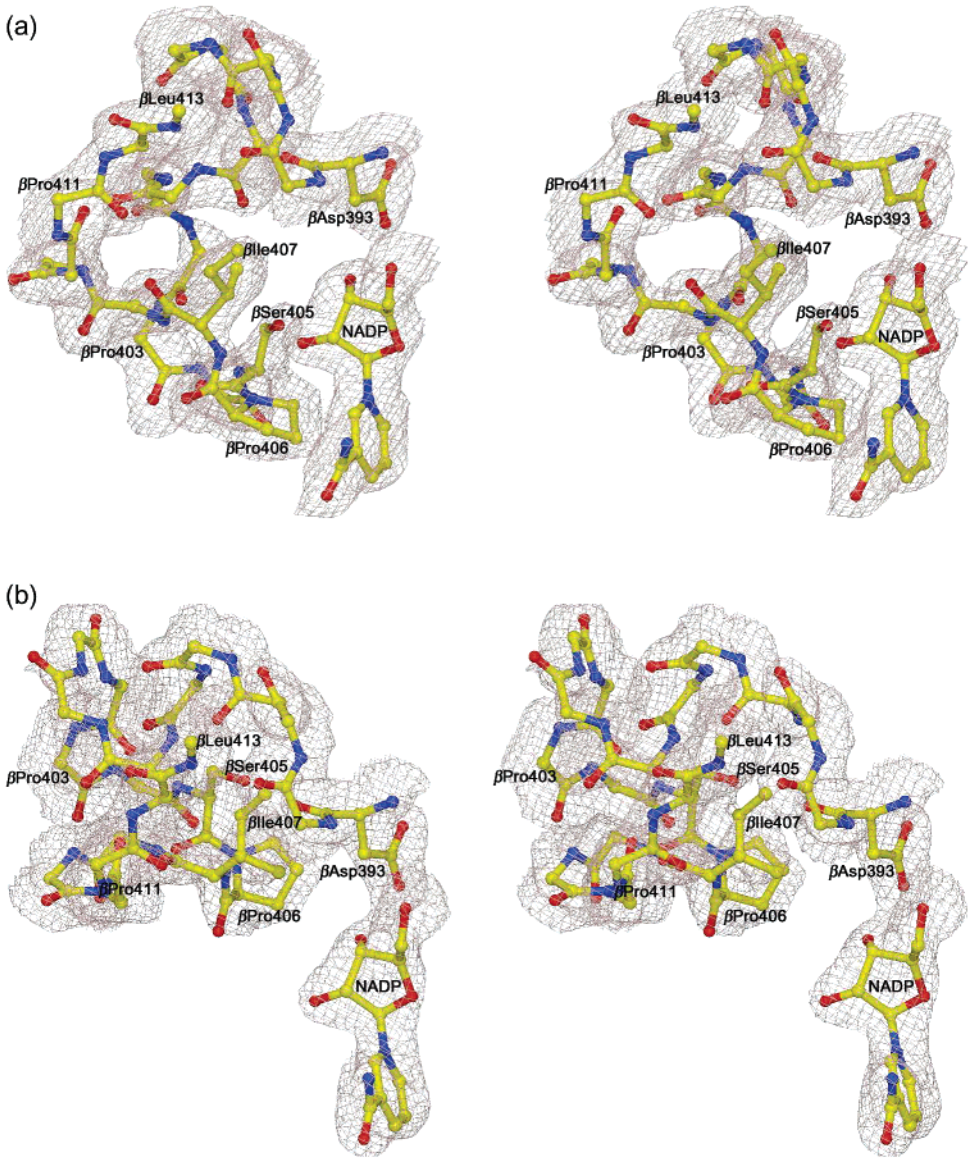

FIGURE 4: Conformational change in loop D. Stereoview of the electron density and models for loop D in (a) the closed conformation, and (b) the open conformation, for the 2.1 Å resolution structures of the NADP complex of dIII. The unbiased σ_A-weighted $2|F_o|-|F_c|$ electron density map, contoured at 1σ, is shown for the nicotinamide nucleoside group of NADP, the main chain of residues βAsp393 to βLeu413, and the side chains of the invariant residue βAsp393 and the conserved residues βSer405, βPro406, and βIle407. Electron density maps for the open and closed conformations of loop D in the NADPH complex at 2.4 Å resolution are very similar.

the side chain. The βHis346 imidazole is a hydrogen bond acceptor with the amide of βVal348 and donor to the carbonyl of βPro411, and these interactions are observed for both the open and closed conformations of loop D (Figure 6b,c). In the open conformation, βHis346 is in a hydrophobic environment due to the adjacent side chains of βPro347, βVal348, βAla349, βLeu373, βVal394, βMet410, βPro411, βIle412, and βLeu413; however, the edge of the imidazole remains exposed to solvent (Figure 6b). In the closed conformation, the environment of βHis346 becomes even more hydrophobic due to the shift in positions of βIle407 and βMet410 (Figure 6a). The Ile side chain moves closer to the imidazole ring to occupy the position of the Met, which in turn moves to shield the edge of imidazole ring from solvent (Figure 6c). Thus, the addition of βIle407 to the immediate environment of βHis346 in the closed conformation of loop D results in the imidazole being buried in a pocket of increased hydrophobicity.

DISCUSSION

TH couples proton-translocation across the membrane to direct hydride transfer between NAD(H) and NADP(H) (eq 1). Reactants and products occur on the same side of the membrane and the difference in redox potentials of NAD(H) and NADP(H) is negligible. It is generally accepted that hydride transfer and proton translocation are coupled to enzyme conformational changes. In the forward reaction, the proton motive force favors a conformation of TH that has increased affinity for NADH and NADP, resulting in hydride transfer. In the reverse reaction conformational change associated with binding of NADPH promotes outward proton translocation (*1*−*4*). Crystal structures of TH dI with and without NAD(H) (*12*, *13*) do not reveal any major conformational changes upon binding or change of oxidation state of NAD(H). Rather, the data indicate that conformational change occurs within dIII (*16*−*20*). Available structures of dIII have been obtained with NADP bound (*9*−*11*, *15*);

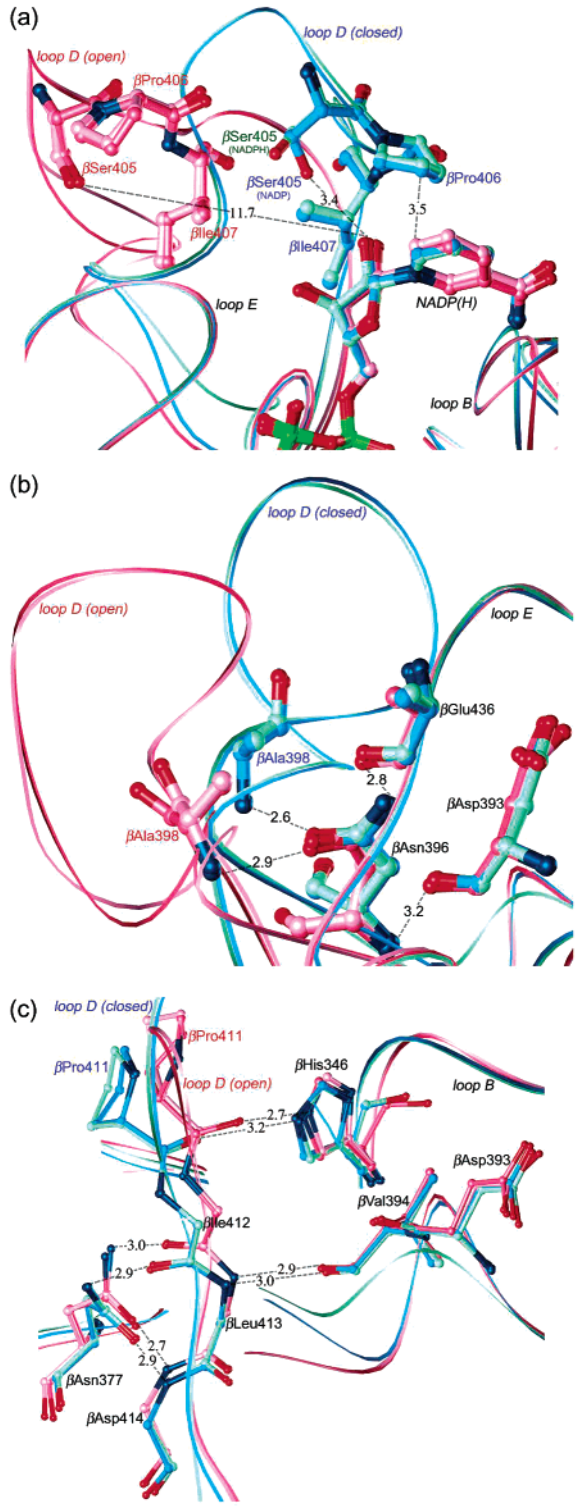

FIGURE 5: Interactions of conserved residues in loop D. (a) The conserved residues βSer405, βPro406, and βIle407 interact with the NADP(H) nicotinamide and ribose in the closed conformation of loop D, but not in the open conformation. A change in the side chain torsion angle of βSer405 is the only significant difference in the oxidized vs. reduced states of the closed form. Relative distances in angstroms in the two conformations are indicated. (b) Interactions of invariant βAsn396 at the N-terminal end of helix $h_{D'}$ and loop D which are retained in both conformations of loop D. (c) Hydrogen bonds involving invariant residues βPro411 on loop D and βHis346 on loop B, and adjacent conserved residues at the C-terminal end of loop D, which are retained in both conformations. The dIII copies are colored: NADP-open (red), NADPH-open (pink), NADP-closed (blue), NADPH-closed (cyan).

however, these structures are all very similar. We set out to obtain a structure of dIII with NADPH bound. A very different "closed" conformation is observed, together with the "open" conformation, confirming the ability of the domain to undergo significant conformational change, and indicating how it occurs. Surprisingly, however, NADPH itself does not affect the conformation compared to NADP. Hence, the crystal structures define four distinct states: NADP-open, NADP-closed, NADPH-open, and NADPH-closed. In the intact enzyme, these states could be associated with the conformational change that is coupled to proton translocation.

Crystallization Conditions. Crystals of *R. rubrum* dIII were obtained from solutions containing H_2O and D_2O in a 1:1 ratio after a number of other approaches were unsuccessful (Experimental Procedures). Transfer of proteins from H_2O to D_2O decreases the enthalpy of unfolding, but stability remains largely unchanged due to entropic compensation (*28*). The higher heat capacity of hydrophobic surfaces (*29*) and increased unfolding transition temperature (*28*) in D_2O can be supposed to induce greater order in exposed hydrophobic surfaces, favoring nucleation and crystal growth. Both NADP and NADPH bound dIII were crystallized from 50% D_2O, but the crystals were obtained at different ionic strengths and temperatures. The structures are isomorphous and single-crystal UV−visible spectra establish the oxidation state for both NADP and NADPH containing crystals (Figure 1b). Given these considerations, we do not expect the presence of D_2O to have affected domain III conformation significantly in comparison to what it would be in H_2O.

Crystal Packing. Some of the interactions between symmetry related molecules involve loop D residues. In particular, the open conformation of one molecule makes crystal packing contacts with the open conformation of another (Figure 7). Molecules that have loop D in the closed conformation do not make mutual crystal packing contacts. Hence, all of the contacts of loop D residues in the closed conformation occur within the asymmetric unit, i.e., to a copy of dIII in the open conformation (Figure 7). The open conformation of loop D has been observed under a variety of conditions (*9*, *10*, *15*) including those employed here. However, the closed conformation has not been observed previously. The occurrence of both conformations in the hexagonal lattice could be related to several factors, including the presence of 50% D_2O, an engineered 22-residue N-terminal sequence (Figure 1a) differing from intact TH, and a 10-residue His-tag within the engineered sequence, which raises the pI of the domain from ~4.75 to ~6.25.

Effect of pH. Another explanation for why the crystals have captured two conformations is that the conditions are relatively acidic; for the NADP bound form the pH is ~6, and for the NADPH bound form the pH is ~6.5 (Experimental Procedures). The initial rate of reverse transhydrogenation between dIII:NADPH and dI:AcPyAD, and the steady state rate of cyclic transhydrogenation, both decrease significantly at low pH with a p*K* of ~5.1 (*19*). Both of these activities are dominated by the rate of hydride transfer, which would be diminished, if not prevented, by the closed conformation of loop D (Figures 2 and 5a). Hence, the closed form of loop D could be more favored at acidic pH, and crystals grown at pH 6−6.5 would grow from a solution containing both conformations. Crystallization of dIII in

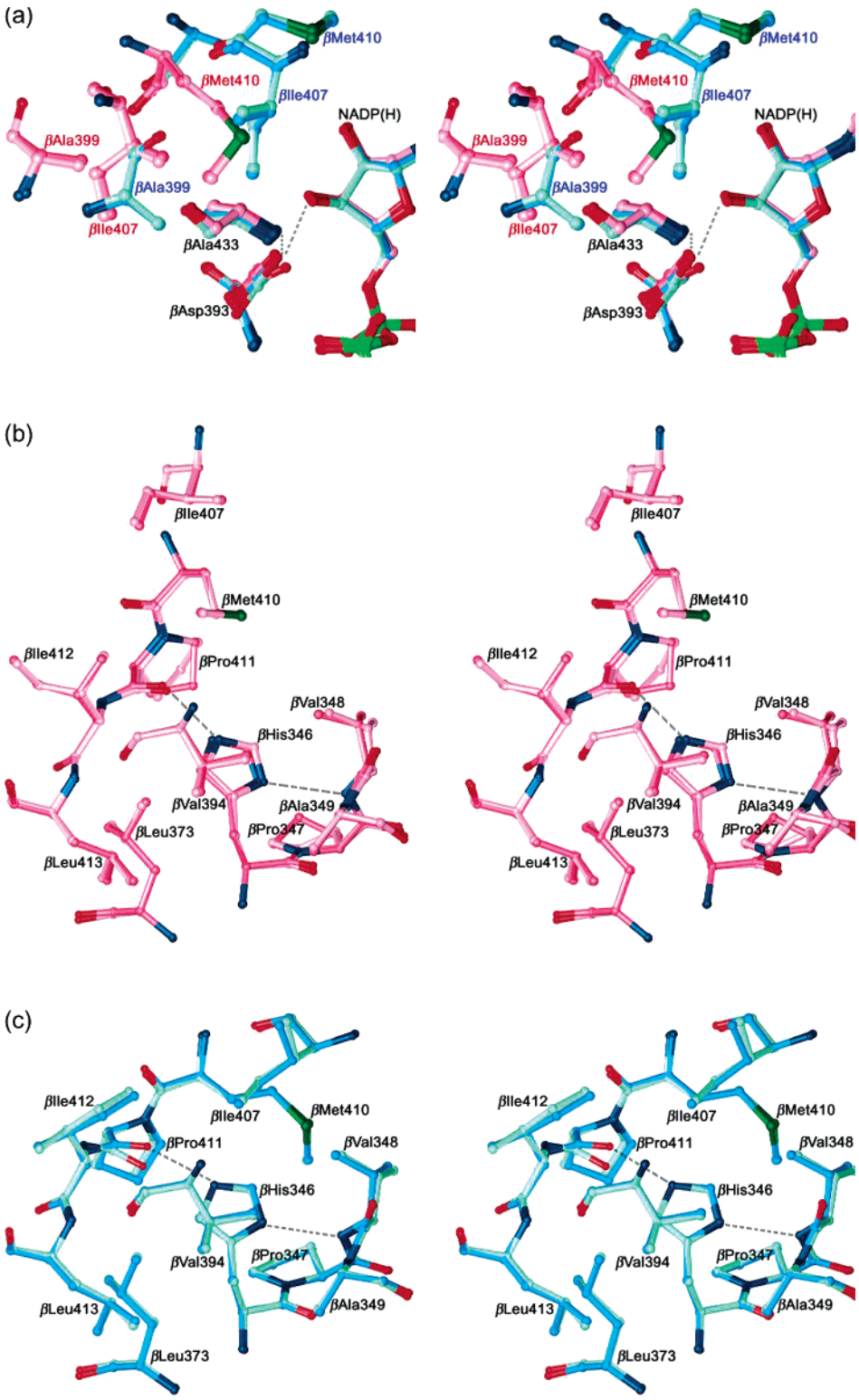

FIGURE 6: Interactions of βAsp393 and βHis346 with respect to the movement of loop D. Stereoviews of the environments of (a) βAsp393 in the open and closed conformations of loop D, (b) βHis346 in the open conformation, and (c) βHis346 in the closed conformation of loop D. The hydrophobic side chains of βAla399, βIle407, and βMet410 shift position with respect to βAsp393 (a), so that βMet410 shields βHis346 from solvent in the closed conformation (c). βHis346 appears to retain two hydrogen bonds with βVal348 and βPro411 in both conformations. The dIII copies are colored as in Figure 5.

exclusively the open conformation of loop D has occurred at pH 7.6 (*9*) and pH 8.2 (*10*). Regardless of the cause, the closed form of loop D results in the highly conserved residues βSer405, βPro406, and βIle407 moving over 10 Å to interact with NADP(H) (Figures 5a and 6a).

Biochemical Studies. The structures are consistent with mutagenesis and labeling studies. Replacement of βSer404 in *E. coli* dIII (βSer405 in *R. rubrum*; Figure S1) with Cys and labeling with MIANS indicates that this side chain is oriented toward the substrate (*18*). This is especially true

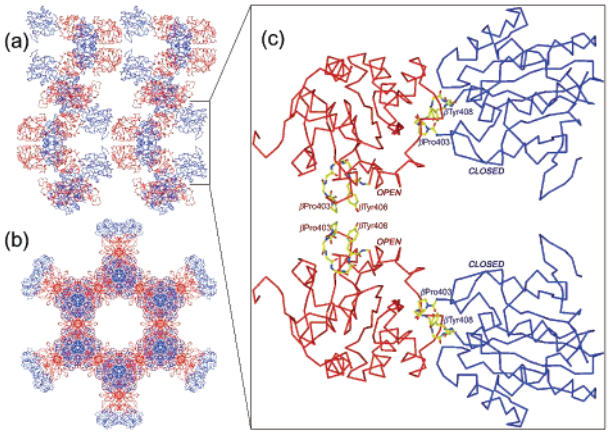

FIGURE 7: Packing diagram for crystals of *R. rubrum* dIII in hexagonal crystals (space group $P6_122$). dIII molecules with loop D in the closed conformation are shown in blue; those in the open conformation are shown in red. The crystal packing diagram viewed along the *x*-axis (a) and along the *z*-axis (b) of the unit cell shows the distribution of solvent channels and intermolecular contacts. Panel (c) shows two adjacent asymmetric units from the view along the *x*-axis that are related by a crystallographic 2-fold axis. The asymmetric unit comprises two molecules of dIII that differ in their loop D conformations. Residues βPro403 and βTyr408 in loop D make packing contacts with corresponding residues in a 2-fold related molecule for the open conformation, but not for the closed conformation.

for the closed conformation of loop D, in which βSer405 is hydrogen bonded to the nicotinamide (Figure 5a). These experiments also showed a role for βIle407 (βIle406 in *E. coli*) in modulating the properties of βAsp393 (*18*), which is in accord with the structures (Figure 6a). Fluorescence resonance energy transfer was used to determine the distance between βGlu416, replaced with tryptophan, and βGly434, replaced with cysteine and labeled with IAEDANS, in *R. rubrum* dIII (*20*). βGly434 is at the apex of loop E, and βGlu416 is in helix $h_{D''}$ at the base of loop D (Figure 2a). The results show that the distance between the two residues increased by 1.3 ± 0.2 Å at pH 5.5 (*20*). The derived distance is consistent with the structures in that loop E essentially does not move in the open vs. closed conformations (Figure 2a,b). However, a small shift in helix $h_{D''}$, observed for the closed conformation (Figure 2a), is consistent with a ~1 Å increase in distance between βGlu416 on this helix and the apex of loop E.

βAsp393 and βHis346. Two invariant, ionizable residues in proximity to NADP(H) are βAsp393 and βHis346 (Figures 6 and S1). These residues are ~9 Å apart on either side of the nicotinamide ribose. βAsp393 is essential for enzyme activity (*30*, *31*). The carboxylate of βAsp393 accepts hydrogen bonds from ribose and the amide of βAla433 (Figure 6a), and interacts with H_2O molecules associated with loop E. The pK_a of βAsp393 may be elevated due to proximity of NADP(H) phosphates (~3.3 Å) and four hydrophobic side chains (Figure 6a). While three of these side chains shift positions upon conformational change, the solvent exposure of βAsp393 remains largely unaffected. Hence, the pK_a of this aspartate may be significantly elevated, but not significantly different in the open vs. closed conformations.

βHis346 resides within a hydrophobic pocket in loop B; eight of nine residues in this loop are invariant (Figures 2a and S1). Substitution of the His in *E. coli* TH with Asn or Gln results in large decreases in both proton translocation and hydride transfer activities (*32*, *33*). The environment of βHis346 becomes even more hydrophobic due to the movement of loop D to the closed form (Figure 6b,c).

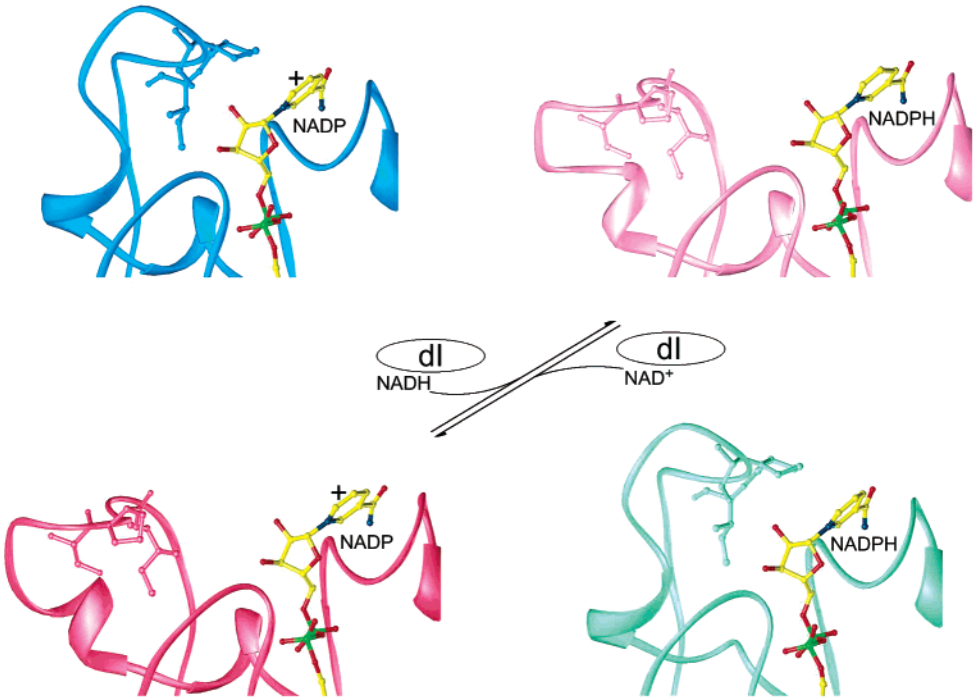

FIGURE 8: Four states of domain III of *R. rubrum* TH are defined by the conformation of loop D and the oxidation state of bound NADP(H). The closed conformation of loop D is shown in blue and green; the open conformation is shown in red and pink (as in Figure 2). All atoms of conserved loop D residues βSer405, βPro406, and βIle407 are shown for each state. Hydride transfer between NADP(H) in domain III and NAD(H) in domain I is expected to occur only in the open conformation; in the closed conformation the nicotinamide ring of NADP(H) is blocked. Each state is unique with respect to net charge on nicotinamide and protein conformation.

Although hydrogen bonding interactions are consistent with the imidazole being unprotonated, the movement of βMet410 could be expected to further lower the pK_a of βHis346. Consequently, the structures indicate that the pK_a of βAsp393 may be elevated while the pK_a of βHis346 may be depressed, consistent with each playing a role in proton uptake or translocation.

Four States of Domain III. The crystal structures of dIII with NADP and NADPH bound reveal that loop D can adopt two conformations (Figure 2a,b), which are observed for both oxidation states (Figure 2c,d). The open conformation of loop D leaves the (dihydro)nicotinamide ring of NADP(H) exposed to solvent while the closed form blocks it (Figure 5a). Apparently, the closed conformation is more favored at the acidic pH of crystallization. A surprising result is that the conformation of dIII is unchanged by the binding of NADP vs. NADPH, contradicting the expectation that NADPH binding induces conformational change as a basis for proton translocation (*1*−*4*). However, if the closed form is protonated relative to the open form, this can be explained. For instance, if βAsp393 is protonated, the structures correspond to (N^+/open, Asp^-), (N^+/closed, Asp), (N/open, Asp^-), and (N/closed, Asp) (where N^+, N are NADP, NADPH, respectively). Each state is unique in terms of electrostatic interaction between the cofactor and the protein while the conformation also differs; this is the essential requirement for function in dIII (Figure 8).

Mechanistic Considerations. In contrast with loop D, only one conformation of loop E is observed in the structures of bovine, human, and *R. rubrum* dIII when NADP(H) is bound (*9*, *10*, *15*; Figure 2). Interactions of conserved loop E residues are retained for both the open and closed forms of loop D with NADP(H) bound (Figures 5b and 6a). Nevertheless, kinetic and mutagenesis experiments focused on the conserved sequence GlyTyrAla at the tip of loop E (βTyr432; Figure S1) indicate that this loop plays an important role in NADP(H) binding and release (*18*). Fluorescence experiments with *R. rubrum* dIII in which the conserved loop E residue βTyr432 was mutated to tryptophan show accelerated rates of release for NADP and NADPH at lower pH (*19*). The absence of change in loop E in crystals at pH ~6, despite large movement in loop D, implies that conformational changes occurring in these loops during turnover in intact TH may be mutually exclusive.

Because the nicotinamide ring is blocked in the closed form, hydride transfer is expected to occur in the open form (Figure 8). In crystals of the "heterotrimeric" dI:dIII complex loop D is in the open conformation and in contact with dI at the conserved "RQD" loop (*15*). This association is modeled to allow direct interaction of NAD(H) and NADP(H) for hydride transfer (*3*). However, superposition of the closed conformation of dIII onto this complex reveals a severe steric clash of loop D with the RQD loop of dI. This would provide a mechanism by which to transmit conformational change from dIII to dI, if following hydride transfer, uptake of a proton within domain III results in the closed conformation.

ACKNOWLEDGMENT

We thank Elizabeth Getzoff for use of her single crystal microspectrophometer, and the staff of the Stanford Synchrotron Radiation Laboratory for generous assistance.

SUPPORTING INFORMATION AVAILABLE

An alignment of dIII residues from 51 prokaryotic and eukaryotic species. This material is available free of charge via the Internet at http://pubs.acs.org.

REFERENCES

1. Hatefi. Y., and Yamaguchi, M. (1992) in *Molecular Mechanisms in Bioenergetics* (Ernster, L., Ed.) pp 265−281, Elsevier, Amsterdam.
2. Hatefi. Y., and Yamaguchi, M. (1996) *FASEB J. 10*, 444−452.
3. Jackson, J. B., White, S. A., Quirk, P. Q., and Venning, J. D. (2002) *Biochemistry 41*, 4173−4185.
4. Bizouarn, T., Althage, M., Pedersen, A., Tigerström, A., Karlsson, J., Johansson, C., and Rydström, J. (2002) *Biochim. Biophys. Acta 1555*, 122−127.
5. Yamaguchi, M., and Hatefi, Y. (1997) *Biochim. Biophys. Acta 1318*, 225−234.
6. Yamaguchi, M., and Hatefi, Y. (1995) *J. Biol. Chem. 270*, 28165−28168.
7. Fjellström, O., Bizouarn, T., Zhang, J.-W., Rydström, J., Venning, J. D., and Jackson, J. B. (1999) *Biochemistry 38*, 415−422.
8. Fjellström, O., Johansson, C., and Rydström, J. (1997) *Biochemistry 36*, 11331−11341.
9. Prasad, G. S., Sridhar, V., Yamaguchi, M., Hatefi, Y., and Stout, C. D. (1999) *Nat. Struct. Biol. 6*, 1126−1131.
10. White, S. A., Peake, S. J., McSweeney, S., Leonard, G., Cotton, N. P. J., and Jackson, J. B. (2000) *Structure 8*, 1−12.
11. Jeeves, M., Smith, K. J., Quirk, P. G., Cotton, N. P. J., and Jackson, J. B. (2000) *Biochim. Biophys. Acta 1459*, 248−257.
12. Buckley, P. A., Jackson, J. B., Schneider, T., White, S. A., Rice, D. W., and Baker, P. J. (2000) *Structure 8*, 809−815.
13. Prasad, G. S., Wahlberg. M., Sridhar, V., Sundaresan, V., Yamaguchi, M., Hatefi, Y., and Stout, C. D. (2002) *Biochemistry 41*, 12745−12754.
14. Yamaguchi, M., and Hatefi, Y. (1993) *J. Biol. Chem. 268*, 17871−17877.
15. Cotton, N. P. J., White, S. A., Peake, S. J., McSweeney, S., and Jackson, J. B. (2001) *Structure 9*, 165−176.
16. Yamaguchi, M., Wakabayashi, S., and Hatefi, Y. (1990) *Biochemistry 29*, 4136−4143.
17. Yamaguchi, M., and Hatefi, Y. (1991) *J. Biol. Chem. 266*, 17020−17025.
18. Johansson, C., Pedersen, A., Karlsson, B. G., and Rydström, J. (2002) *Eur. J. Biochem. 269*, 4505−4515.
19. Rodrigues, D. J., Venning, J. D., Quirk, P. G., and Jackson, J. B. (2001) *Eur. J. Biochem. 268*, 1430−1438.
20. Rodrigues, D. J., and Jackson, J. B. (2002) *Biochim. Biophys. Acta 1555*, 8−13.
21. Stura, E. A., Nemerow, G. N., and Wilson, I. A. (1992) *J. Cryst. Growth 122*, 273−285.
22. Leslie, A. G. W. (1994) *Acta Crystallogr. D50*, 760−763.
23. Read, R. J. (2001) *Acta Crystallogr. D57*, 1373−1382.
24. Brünger, A. T., Adams, P. D., Clore, G. M., DeLano, W. L., Gros, P., Grosse-Kunstleve, R. W., Jiang, J.-S., Kuszewski, J., Nilges, M., Pannu, N. S., Read, R. J., Rice, L. M., Simonson, T., and Warren, G. L. (1998) *Acta Crystallogr. D54*, 905−921.
25. McRee, D. E. (1999) *J. Struct. Biol. 125*, 156−165.
26. Bourgeois, D., Vernede, X., Adam, V., Fioravanti, E., and Ursby, T. (2002) *J. Appl. Crystallogr. D54*, 905−921.
27. Bellamacina, C. R. (1996) *FASEB J. 10*, 1257−1269.
28. Makhatadze, G. I., Clore, G. M., and Gronenborn, A. M. (1995) *Nat. Struct. Biol. 2*, 852−855.
29. Lopez, M. M., and Makhatadze, G. I. (1998) *Biophys. Chem. 74*, 117−125.
30. Fjellström, O., Axelsson, M., Bizouarn, T., Hu, X., Johansson, C., Meuller, J., and Rydström, J. (1999) *J. Biol. Chem. 274*, 6350−6359.
31. Bergkvist, A., Johansson, C., Johansson, T., Rydström, J., and Karlsson, B. G. (2000) *Biochemistry 39*, 12595−12605.
32. Bragg, P. D., and Hou, C. (1996) *Eur. J. Biochem. 241*, 611−618.
33. Bragg, P. D., Glavas, N. A., and Hou, C. (1997) *Arch. Biochem. Biophys. 338*, 57−66.

BI035006Q